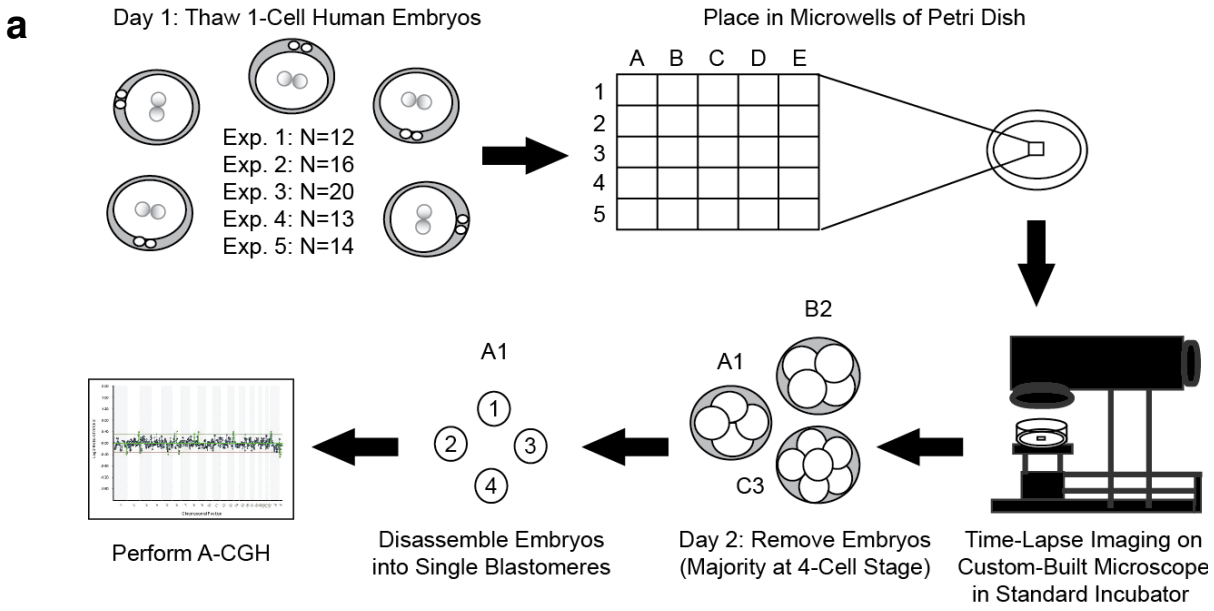

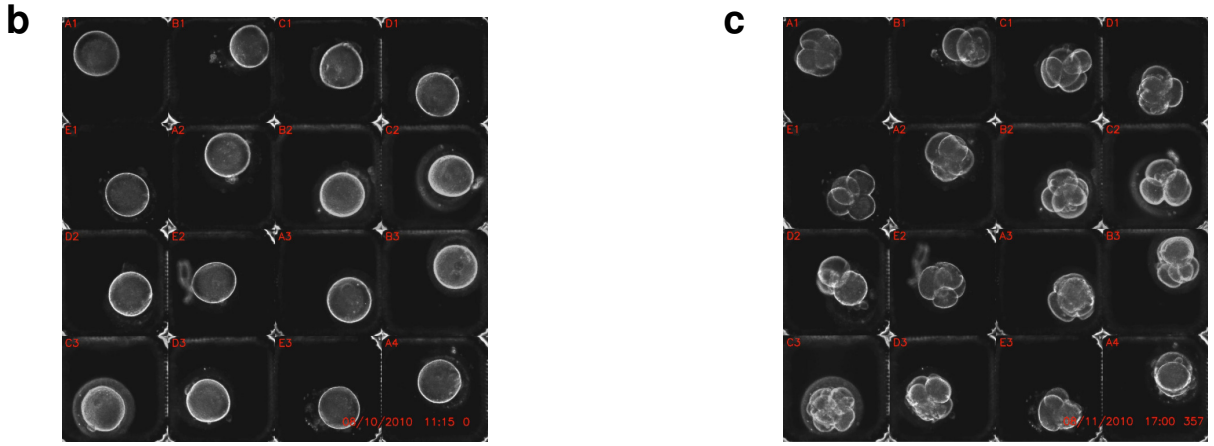

Supplementary Figure S1. Experimental design of embryonic aneuploidy experiments using time-lapse image and chromosome analysis. (a) The development of 75 embryos at the 1-cell (2 pronuclear; 2PN) stage was tracked in five separate experiments. For each experimental set, human zygotes were thawed on day 1 and cultured together in alphabetically and numerically labeled microwell containing petri dishes. Time-lapse imaging, using a custom-built microscope with dark-field illumination placed in a standard incubator, was performed until day 2 (approximately 30 hours). Once the majority had reached the 4-cell stage, the embryos were removed and dissembled into single blastomeres using the microwell labels for embryo identification. The chromosomal complement of each blastomere was evaluated by Array-Comparative Genomic Hybridization (A-CGH), the results of which were correlated with embryo imaging behavior by manually measuring dynamic imaging parameters between the first **(b)** and last **(c)** frame of an image sequence compiled into a time-lapse movie (Supplementary Movie 1) with well identification labels and time stamps.

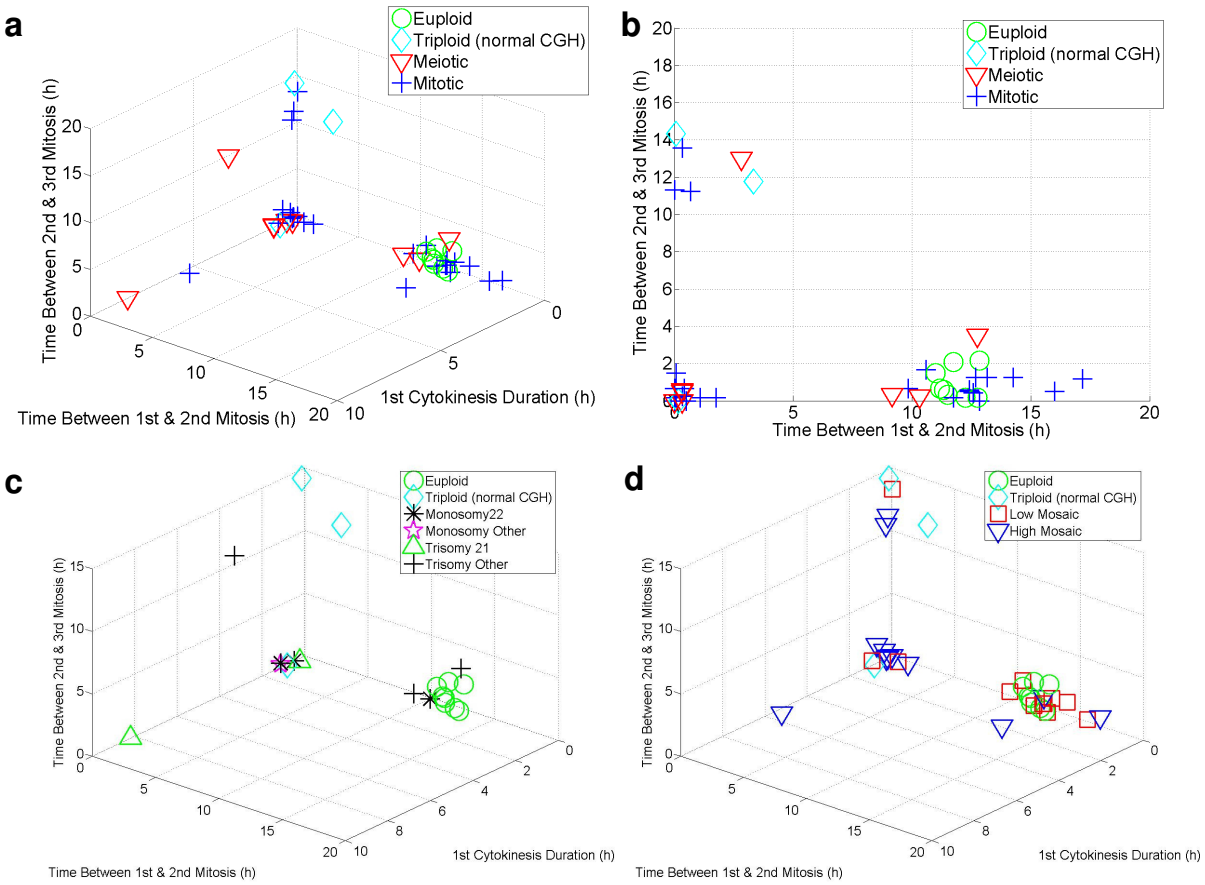

Supplementary Figure S2. Differential clustering of euploid embryos and embryos with meiotic and mitotic errors. (a) 3-Dimensional (3-D) parameter plot demonstrating the separation of euploid embryos (green circles) from triploid embryos (aqua diamonds) and embryos with meiotic errors (red triangles) and partial overlap of embryos with mitotic errors (blue plus signs); n=45 **(b)** The 2-D parameter plot of euploid, triploid and meiotic/mitotic error embryos illustrated in **a.** **(c)** A similar plot of euploid, triploid, monosomy 22 (black asterisks), monosomy other (pink stars), trisomy 21 (green triangles) and trisomy other (black plus signs) embryos showing the distinction between euploid embryos and those with different meiotic errors; n=20 **(d)** Further examination of the relationship between euploid, triploid, high (blue triangles) or low (red squares) mosaic mitotic embryos by 3-D parameter plotting reveals that the overlap between euploid and mitotic error embryos are predominantly those with low mosaicism; n=36.

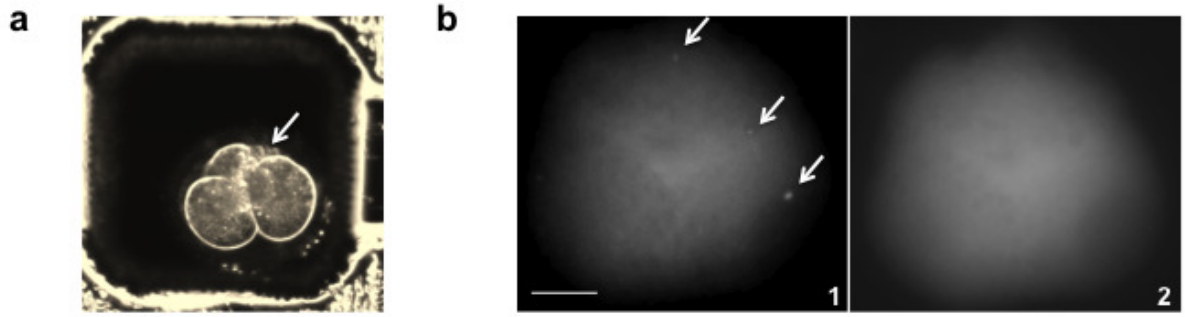

Supplementary Figure S3. Detection of chromosome copy number in triploid human embryos by FISH. (a) The last frame in an imaging sequence of an embryo with fragmentation (indicated by the white arrow) that appeared to be triploid based on imaging parameter assessment. **(b)** Fluorescent *In Situ* Hybridization (FISH) analysis of a blastomere from the embryo pictured in **a** showing three copies of chromosome 18 (1; indicated by white arrows) to confirm the embryo as triploid and female since no signals for the Y-chromosome (2) were detected. Scale bar, 10μm.

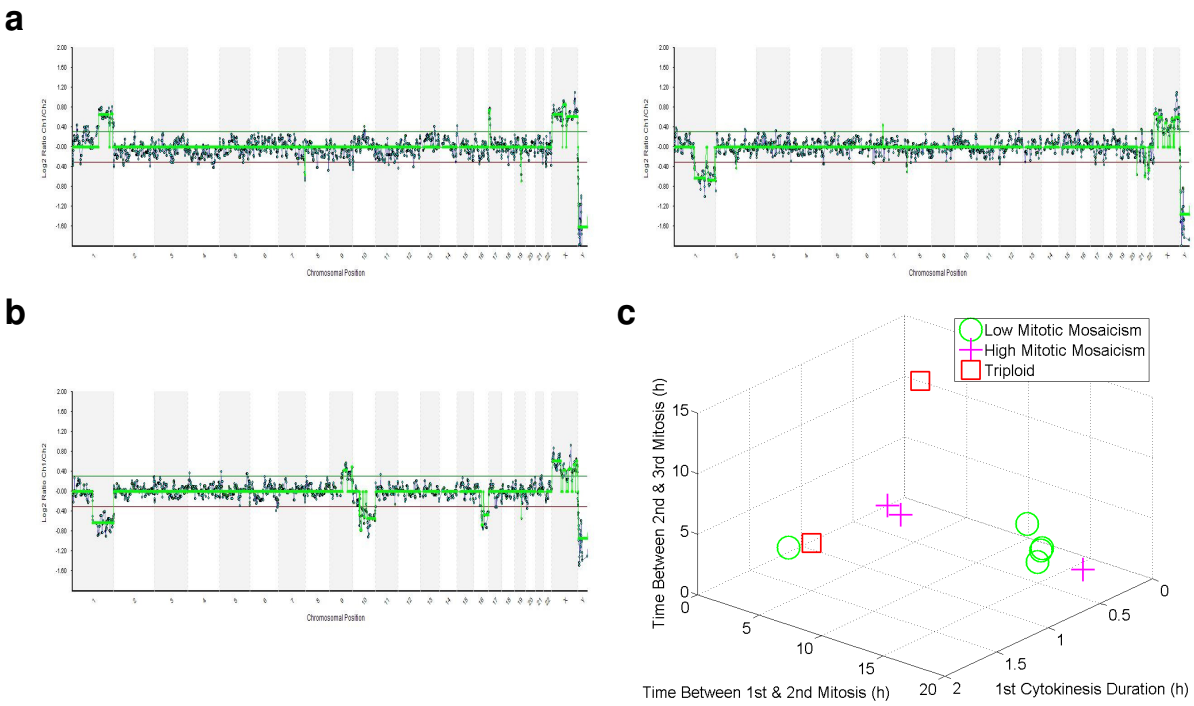

Supplementary Figure S4. Parameter timing of aneuploid embryos with additional sub-chromosomal errors. (a) A-CGH profiles of an aneuploid embryo with a balanced partial loss and gain of chromosome 1q between two blastomeres that did not exhibit fragmentation. **(b)** An A-CGH profile of an individual blastomere from an embryo with fragmentation showing a partial loss of chromosome 1q, partial gain of chromosome 9q, partial loss of chromosome 10q and a partial loss chromosome 16q. **(c)** 3-Dimensional (3-D) parameter plot showing the cell cycle parameter timing of low mitotic mosaic (green circles), high mitotic mosaic (pink plus signs) and triploid embryos (red squares) that also exhibited either balanced or unbalanced chromosomal losses and/or gains depicted in Supplementary Table S4; n=10.

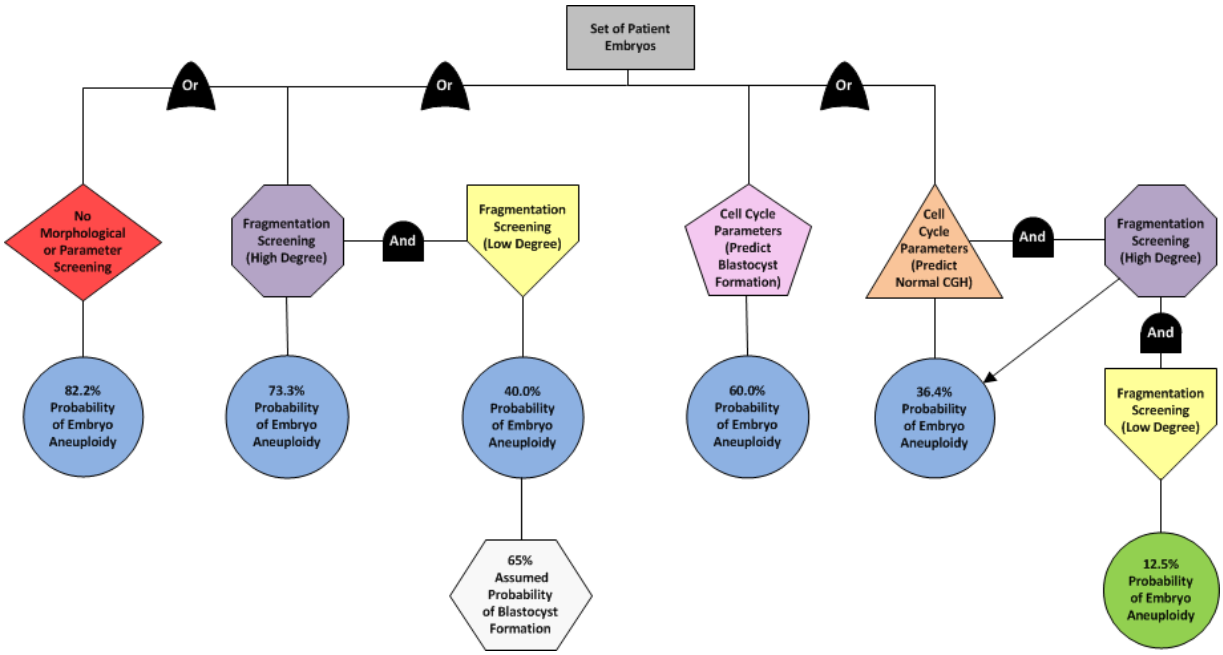

Supplementary Figure S5. Assessment of risk of embryonic euploidy versus aneuploidy. Risk tree showing the probability of embryonic euploidy (blue or green circles) if no morphological or parameter screening (red diamond), high fragmentation screening (purple octagon), low fragmentation screening (yellow pentagon), cell cycle parameters that predict blastocyst formation (pink pentagon) and cell cycle parameters that predict normal CGH (orange triangles) were used to assess developmental competence. The probability of embryonic euploidy in the absence of morphological or parameter assessment, or essentially the chances of obtaining an aneuploid embryo at random, is 17.8%, which is in agreement with Vanneste *et al*. (Supplementary Table S5)[5]. By triaging embryos via high and low fragmentation as a screening tool, this percentage increased to 26.7% and 60%, respectively. However, only 65% of the embryos assessed via fragmentation screening alone exhibited timing values that would be predictive of blastocyst formation (white hexagon), indicating that fragmentation alone is not sufficient for the prediction of embryo viability (Fig. 3c). Using our previously defined cell cycle parameter timing windows to predict blastocyst formation[1], the probability of embryonic euploidy in the present study is 40% and if the refined parameter timing windows that predict normal chromosome complement as determined in this study were applied, this percentage increased to 63.6%. Finally, when fragmentation assessment was implemented in conjunction with cell cycle parameter analysis, the probability of embryonic euploidy increased to 87.5% (Supplementary Table S5).

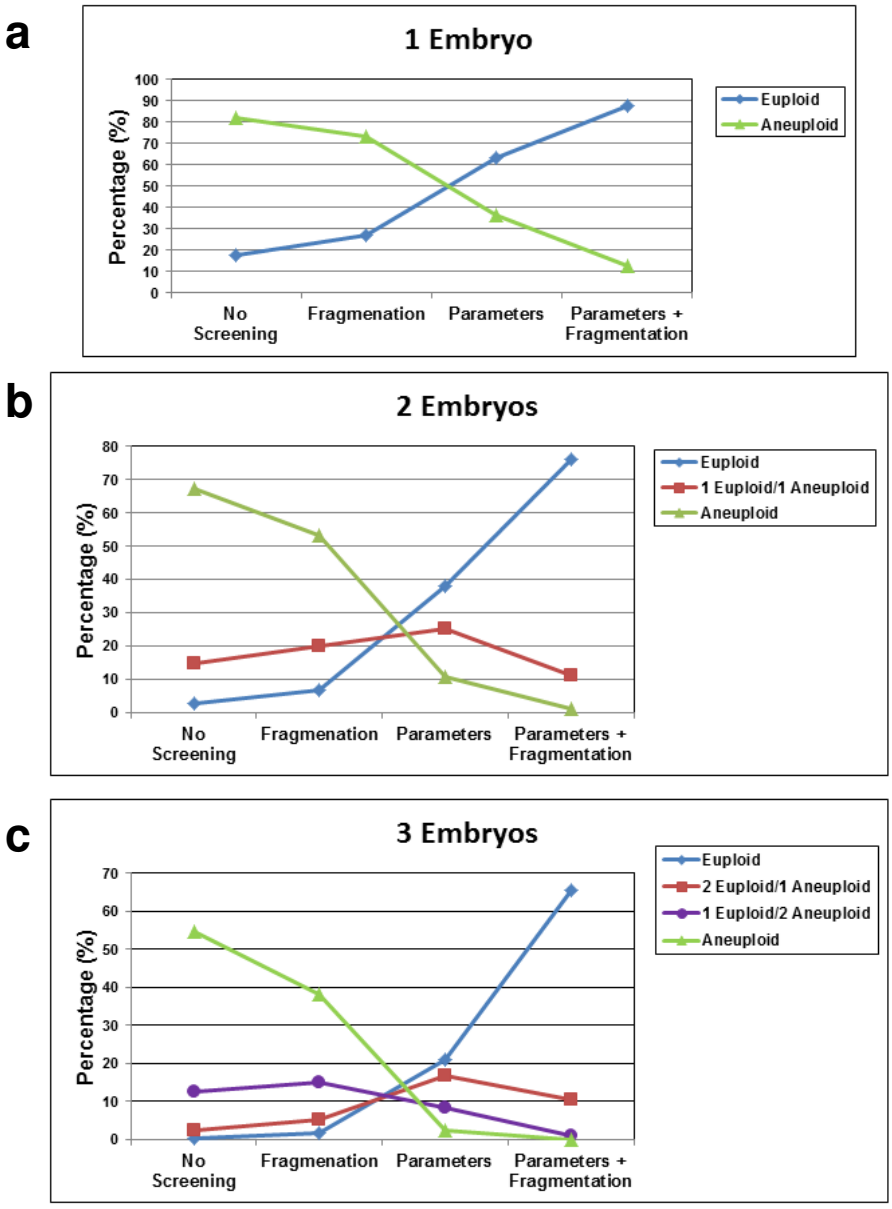

Supplementary Figure S6 Graphic representation of the probability of embryonic euploidy versus aneuploidy with single or multiple embryo transfer. Graphs representing the calculated results in Table S6 are used to illustrate the probability of embryonic euploidy versus aneuploidy when **(a)** 1 embryo **(b)** 2 embryo or **(c)** 3 embryos were selected for patient transfer using only high fragmentation assessment since according to current clinical practice, embryos with greater than 25% fragmentation by cytoplasmic volume on day 3 are graded as poor quality and associated with significantly decreased live birth rates[16]. Analogous to the findings observed with single embryos, fragmentation screening alone had minimal effect on the probability of embryonic aneuploidy in comparison to the cell cycle parameters or the parameters in combination with both high and low fragmentation assessment when a 2- or 3-embryo transfer scenario was used.

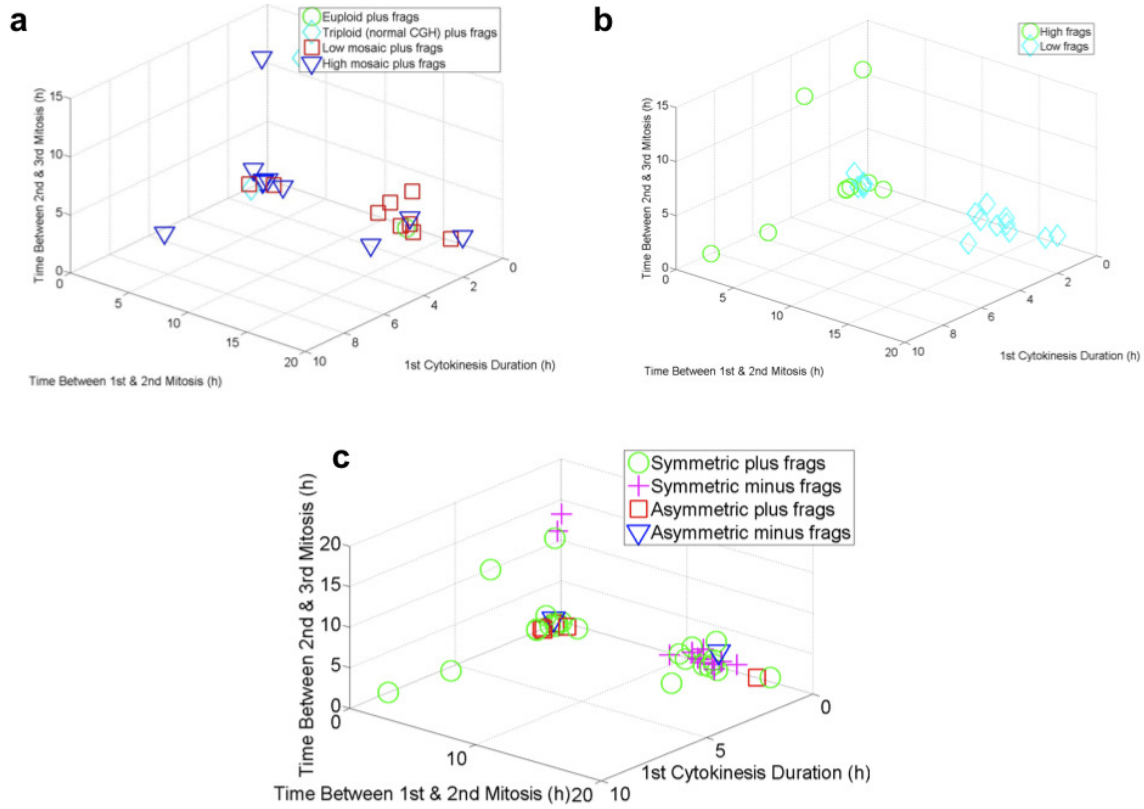

Supplementary Figure S7. Assistance of additional fragmentation criteria in the assessment of developmental competence. (a) 3-Dimensional (3-D) plot showing the relationship between euploid (green circles), triploid (aqua diamonds), high (blue triangles) or low (red squares) mosaic mitotic embryos and fragmentation. Of the embryos with mitotic errors that exhibited fragmentation, 5 out of 9 and 1 out of 11 embryos that clustered in a region similar to that of euploid embryos had underlying low mosaic and high mosaic mitotic errors, respectively; n=23 **(b)** An examination of high (green circles) and low (aqua diamonds) fragmentation by 3-D plotting reveals that all highly fragmented embryos exhibit abnormal parameter timing. A high degree of fragmentation was measured as more than 25% fragmentation by volume of cytoplasm and a low degree of fragmentation was measured as less than 25% fragmentation by volume of cytoplasm. **(c)** 3-D parameter plot of embryos with symmetrical blastomeres plus (green circles) or minus (pink plus signs) fragmentation and those embryos exhibiting blastomere asymmetry with (red squares) and without (blue triangles) fragments. Note that asymmetrical embryos are more likely to be fragmented and have abnormal parameter timing; n=45.

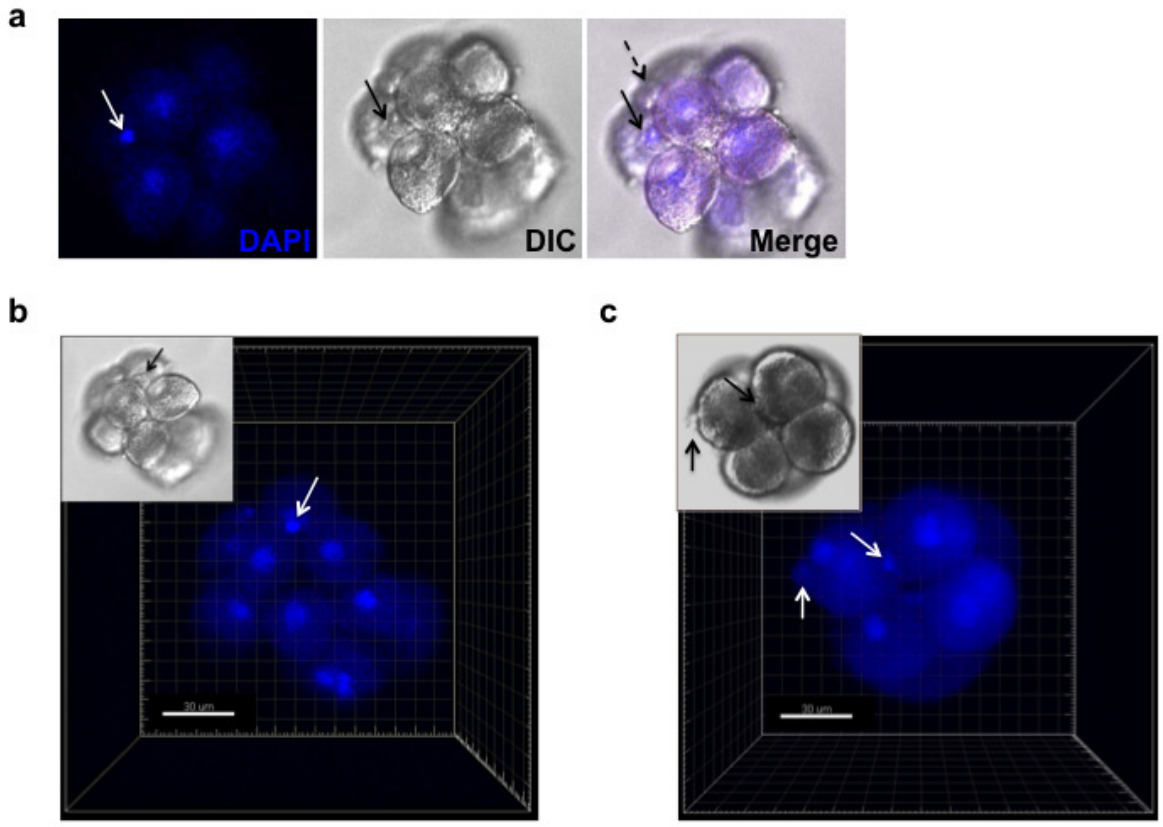

Supplementary Figure S8 Further examples of nuclear DNA within cellular fragments of cleaving human embryos. (a) Single confocal image frame of a zona pellucida-free cleavage-stage embryo with cellular fragmentation (indicated by black arrows) visualized by Differential Interference Contrast (DIC) showing positive DAPI signals (indicated by white solid arrow) in a fragment (indicated by a solid black arrow) adjacent to a DAPI-negative fragment (indicated by a dashed black arrow). **(b)** 3-D modeling of an embryo with fragments imaged by DIC (left) and Z-stack confocal microscopy (right) exhibiting one and **(c)** two DAPI positive fragments, respectively. Scale bar, 30µm.

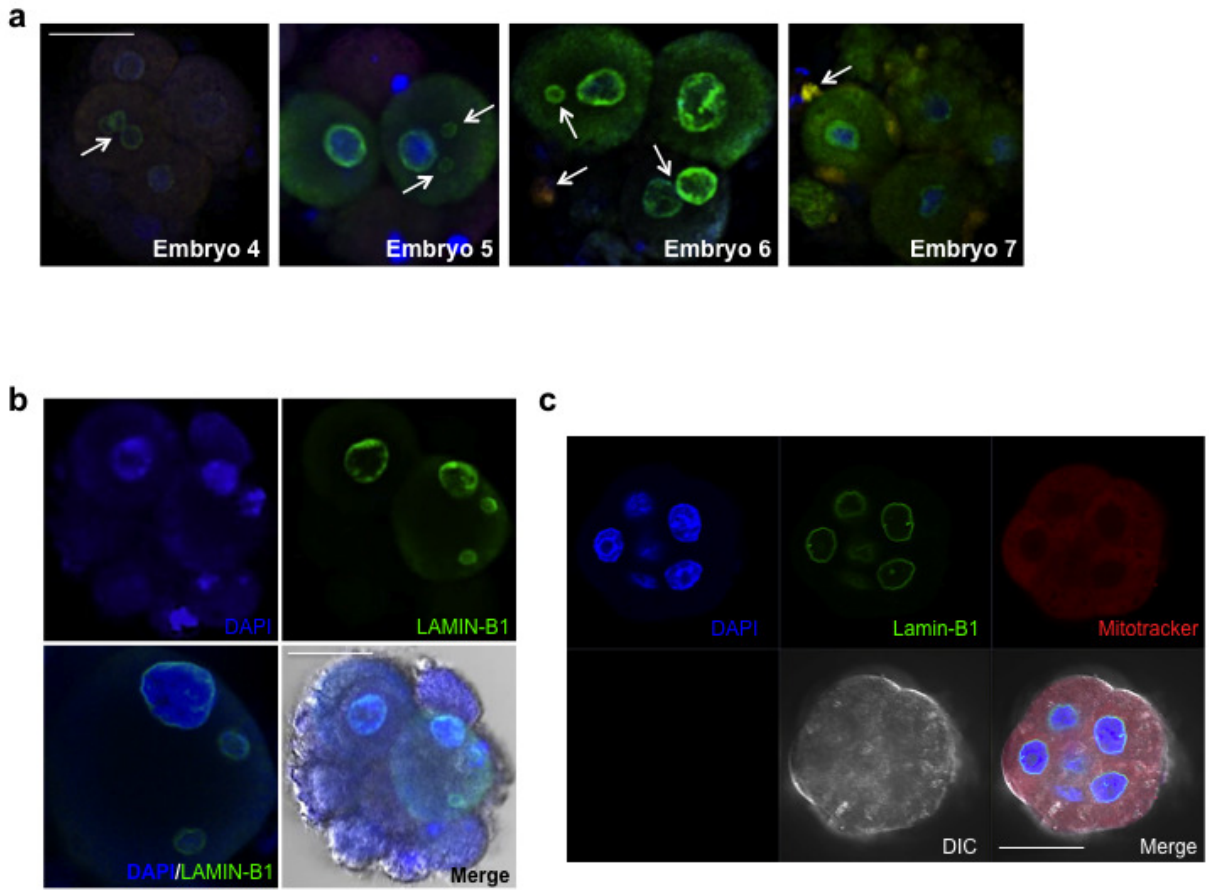

Supplementary Figure S9 Additional evidence of embryonic micronuclei in the blastomeres of only human embryos. **(a)** Confocal imaging of LAMIN-B1 (green) and CENP-A (orange) expression in DAPI-stained (blue) cleavage-stage human embryos showing the appearance of embryonic micronuclei and/or chromosome-containing fragments. **(b)** Similar imaging analysis for LAMIN-B1 expression in another DAPI-stained embryo also visualized by DIC. Note the presence of micronuclei enapasulated by LAMIN-B1 expression in the blastomeres of human embryos, but not **(c)** mouse embryos also stained with Mitotracker Red. Scale bar, 50μm.

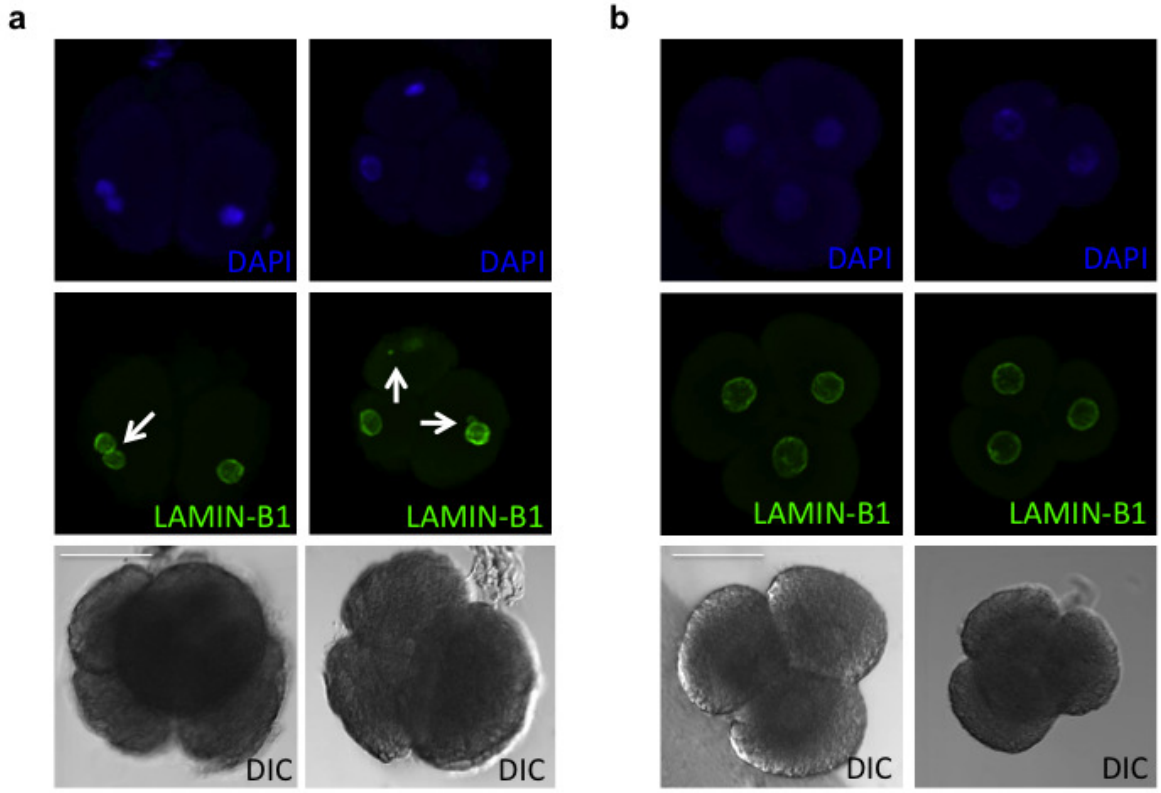

Supplementary Figure S10. Detection of micronuclei in embryos with normal and abnormal parameter timing. (a) Confocal imaging of LAMIN-B1 (green) in additional DAPI-stained (blue) and DIC visualized human embryos with **(a)** abnormal and **(b)** normal cell cycle parameters plotted in Figure 4e. Scale bar, 50µm.

Parameter Measurements	Normal CGH (N=8)	Meiotic Error (N=9)	Mitotic Error (N=25)	High Mosaic Mitotic Error (N=13)	Low Mosaic Mitotic Error (N=12)
Duration of first cytokinesis	14.4±4.2 Min.	117.2±166.5 Min.	36.0±66.9 Min.	52.7±89.8 Min.	17.9±16.8 Min.
Time between first and second mitosis	11.8±0.71 Hours	4.0±5.2 Hours*	6.4±6.6 Hours*	3.5±6.2 Hours**	9.6±5.6 Hours
Time between second and third mitosis	0.96±0.84 Hours	2.0±4.3 Hours	2.0±3.9 Hours	2.2±4.1 Hours	1.8±3.8 Hours

Supplementary Table S1. Individual cell cycle parameter analysis in euploid and aneuploid embryos. Comparison of the individual parameter values and standard deviations between embryos with normal CGH profiles (n=8), meiotic (n=9, *=$p<0.05$ by ANOVA; $p=0.06$ by Kruskal-Wallis), and mitotic (n=25, *=$p<0.05$ by ANOVA; $P=0.08$ by Kruskal-Wallis) errors and embryos with high (n=13, **=$p<0.01$ by ANOVA; *=$p<0.05$ by Kruskal-Wallis) or low (n=12) mitotic mosaicism. The mean values and standard deviations of embryos that were determined to be chromosomally normal by A-CGH can be used to potentially refine the parameters predictive of blastocyst formation.

a

Ch.	1	2	3	4	5	6	7	8	9	10	11	12	13	14	15	16	17	18	19	20	21	22	Sex
B1	2	2	2	2	2	2	2	2	2	2	2	2	2	2	2	2	2	2	2	2	2	2	XX
B2	2	2	2	2	2	1	2	2	2	2	2	2	2	2	2	2	2	2	2	2	2	2	XX
B3	2	2	2	2	2	1	2	2	2	2	2	2	2	2	2	2	2	2	2	2	2	2	XX
B4	2	2	2	2	2	2	2	2	2	2	2	2	2	2	2	2	2	2	2	2	2	2	XX
Sum	8	8	8	8	8	6	8	8	8	8	8	8	8	8	8	8	8	8	8	8	8	8	8

b

Ch.	1	2	3	4	5	6	7	8	9	10	11	12	13	14	15	16	17	18	19	20	21	22	Sex
B1	2	2	2	2	2	2	2	2	2	2	2	2	2	2	2	2	2	2	2	2	3	2	XX
B2	2	2	2	2	2	2	2	2	2	2	2	2	2	2	2	2	2	2	2	2	2	2	XX
B3	2	2	2	2	2	2	2	2	2	2	2	2	2	2	2	2	2	2	2	2	2	2	XX
B4	2	2	2	2	2	2	2	2	2	2	2	2	2	2	2	2	2	2	2	2	1	2	XX
Sum	8	8	8	8	8	8	8	8	8	8	8	8	8	8	8	8	8	8	8	8	8	8	8

c

Ch.	1	2	3	4	5	6	7	8	9	10	11	12	13	14	15	16	17	18	19	20	21	22	Sex
B1	2	2	2	2	1	2	2	2	2	2	2	2	2	2	2	2	2	2	2	2	2	2	XY
B2	2	2	1	2	1	2	2	2	2	2	2	2	2	2	1	1	2	2	2	2	2	2	XY
B3	2	2	2	2	3	2	2	2	2	2	2	2	2	2	2	2	2	2	2	2	2	2	XY
B4	2	2	2	2	2	2	2	2	2	2	2	2	2	2	3	3	2	2	2	2	2	2	XY
Sum	8	8	7	8	7	6	8	8	8	8	8	8	8	8	8	8	8	8	8	8	8	8	8

d

Ch.	1	2	3	4	5	6	7	8	9	10	11	12	13	14	15	16	17	18	19	20	21	22	Sex
B1	1	2	2	2	2	2	2	2	2	1	2	2	2	2	2	1	2	2	2	2	2	2	XX
B2	3	2	2	2	2	2	2	2	2	1	2	2	2	2	2	1	2	2	2	2	2	2	XX
B3	1	2	2	2	2	2	2	2	2	1	2	2	2	2	2	1	2	2	2	2	2	2	XX
B4	1	2	2	2	2	2	2	2	2	3	2	2	2	2	2	3	2	2	2	2	2	2	XX
Sum	6	8	8	8	8	8	8	8	8	6	8	8	8	8	8	6	8	8	8	8	8	8	8

e

Ch.	1	2	3	4	5	6	7	8	9	10	11	12	13	14	15	16	17	18	19	20	21	22	Sex
B1	3	1	3	1	2	2	2	2	1	2	2	2	3	2	2	2	2	3	2	3	2	1	X
B2	2	3	2	2	2	3	1	1	2	1	2	2	2	2	2	2	2	1	2	2	2	2	XX
B3	2	2	1	1	1	3	2	2	2	2	2	2	2	2	2	2	1	3	2	1	2	2	XX
B4	1	1	2	3	2	2	2	2	2	2	1	3	2	2	3	3	3	1	2	3	1	2	XX
B5	2	1	3	2	2	2	2	2	1	2	2	2	3	2	2	1	2	3	2	3	2	2	X
B6	2	2	1	2	2	2	2	2	2	2	2	2	2	2	2	2	1	3	2	1	2	2	XX
Sum	12	10	12	11	11	14	11	11	10	11	11	13	14	12	13	12	11	14	12	13	11	11	10

Supplementary Table S2. Comparison of chromosome composition in aneuploid embryos with simple and complex mitotic errors. Full chromosome analysis of a **(a)** fragmented and **(b)** non-fragmented 4-cell embryo pictured in Figure 2a (left and right, respectively), showing that the aneuploid embryo with fragmentation is missing 2 copies of chromosome 6 from two of its blastomeres. **(c)-(e)** The chromosomal status of all blastomeres in additional embryos with mitotic errors that exhibit chromosomal losses or gains as well as atypical chromosomal ratios that are inconsistent with mitotic non-disjunction. Note that only 2 chromosomes are unaffected in the blastomeres of the embryo depicted in **e**, which is likely to have incurred both meiotic and mitotic errors.

Embryo Number	Aneuploidy Type	Sub-Chromosomal Analysis	Fragmentation Analysis
1	Low mitotic mosaicism	Unbalanced partial gain Ch. 10p	Yes
2	Low mitotic mosaicism	Balanced partial loss/gain Ch. 1q	No
3	High mitotic mosaicism	Unbalanced partial loss Ch. 10q	Yes
4	Low mitotic mosaicsim	Unbalanced partial loss Ch.1q, 10q and 16q and partial gain Ch.9q	Yes
5	High mitotic mosaicism	Unbalanced partial loss Ch.8p, 1q and 12q	Yes
6	High mitotic mosaicism	Unbalanced partial loss Ch.9q and partial gain Ch.1q, 7p, 10q and 16q	Yes
7	Low mitotic mosaicsim	Unbalanced partial gain Ch. 11q	Yes
8	Low mitotic mosaicism	Unbalanced partial loss Ch.6q and 7p	Yes
9	Triploid	Unbalanced partial gain Ch. 22q	Yes
10	Triploid	Unbalanced partial gain Ch. 19p	Yes

Supplementary Table S3. Sub-chromosomal losses and gains in several aneuploid embryos. A table depicting the sub-chromosomal analysis of certain low/high mitotic mosaic and triploid embryos with cell cycle parameter timing illustrated in Supplementary Figure S4. Note that one of these embryos had a balanced translocation between blastomeres and it is the only embryo that did not exhibit cellular fragmentation.

	Euploid With Cellular Fragments	Aneuploid With Cellular Fragments	Triploid With Cellular Fragments	Meiotic Error With Cellular Fragments	Meiotic Error Without Cellular Fragments	Meiotic Error Begin Fragmenting 1-Cell Stage	Meiotic Error Begin Fragmenting 2-4 Cell Stage	Mitotic Error With Cellular Fragments	Mitotic Error Without Cellular Fragments	Mitotic Error Begin Fragmenting 1-Cell Stage	Mitotic Error Begin Fragmenting 2-4 Cell Stage
Number of Embryos	1	28	3	9	0	8	1	19	6	5[#]	14
Total Number of Embryos	8	34	3	9	9	9	9	25	25	19	19
Percentage	12.5%	82.4%	100%	100%	0%	89%	11%	76%	24%	26%	74%

Supplementary Table S4. Correlation between embryo ploidy and the incidence and timing of cellular fragmentation. A table depicting the correlation between the number and percentage of euploid, aneuploid or triploid human embryos and the incidence and timing of cellular fragmentation. [#]Note that the 5 embryos, which begin fragmenting at the 1-cell stage, were also characterized by complex mitotic mosaicism, suggesting that these embryos likely acquired a meiotic error followed by a mitotic error.

Measurement (morphological and/or parameter analysis)	Calculation (# of euploid/total # of embryos)	Percentage (probability of embryo euploidy)	Literature Reference
No morphological or parameter screening	8/45	17.8%	Present study and Vanneste *et al.* 2009
Fragmentation (high degree)	12/45	26.7%	Present study and Antczak & Van Blerkom, 1999
Fragmentation (high & low degree)	27/45	60%	Present study and Antczak & Van Blerkom, 1999
Cell cycle parameters that predict blastocyst formation	8/20	40%	Present study and Wong/Loewke *et al.* 2010
Cell cycle parameters that predict normal CGH	7/11	63.6%	Present study
Cell cycle parameters that predict normal CGH plus fragmentation (high degree)	7/11	63.6%	Present study
Cell cycle parameters that predict normal CGH plus fragmentation (high & low degree)	7/8	87.5%	Present study

Supplementary Table S5. Calculation of embryonic euploidy versus aneuploidy risk. The table shows the calculation (number of euploid embryos/total number of embryos), the resulting probability of embryonic euploidy expressed as a percentage and the supporting literature reference for each morphological and/or parameter assessment illustrated in Supplementary Figure S5. Note that the highest percentage of embryonic euploidy would be obtained with the combination of cell cycle parameters that predict normal A-CGH and high/low fragmentation analysis.

# of Embryos Transferred	No Morphological or Parameter Screening	Fragmentation Assessment in Current Clinical Practice (High Degree)	Cell Cycle Parameters that Predict Normal CGH	Cell Cycle Parameters that Predict Normal CGH Plus Fragmentation Assessment (High & Low Degree)
1	Euploid=17.8%	Euploid=26.7%	Euploid=63.6%	Euploid=87.5%
2	Both Euploid=2.8% 1 Euploid/1 Aneuploid=14.9% Both Aneuploid=67.3%	Both Euploid=6.7% 1 Euploid/1 Aneuploid=20.0% Both Aneuploid=53.3%	Both Euploid=38.2% 1 Euploid/1 Aneuploid=25.4% Both Aneuploid=10.9%	Both Euploid=76.1% 1 Euploid/1 Aneuploid=11.4% Both Aneuploid=1.1%
3	All Euploid=0.4% 2 Euploid/1 Aneuploid=2.4% 1 Euploid/2 Aneuploid=12.5% All Aneuploid=54.7%	All Euploid=1.6% 2 Euploid/1 Aneuploid=5.1% 1 Euploid/2 Aneuploid=14.9% All Aneuploid=38.4%	All Euploid=21.2% 2 Euploid/1 Aneuploid=17.0% 1 Euploid/2 Aneuploid=8.5% All Aneuploid=2.4%	All Euploid=65.7% 2 Euploid/1 Aneuploid=10.4% 1 Euploid/2 Aneuploid=1.0% All Aneuploid=0.05%

Supplementary Table S6. Probability of embryonic euploidy versus aneuploidy with single or multiple embryo transfer. A table demonstrating the probability of embryonic euploidy and aneuploidy in a scenario, whereby 1, 2 or 3 embryos were selected for patient transfer based on no or different morphological and/or parameter screening. The percentages in the table correspond to Supplementary Figure S6. Note that the calculated values of embryonic euploidy with high fragmentation screening for 1, 2 or 3 embryos are congruent with observed values as reported percentages of both single and multi-fetus pregnancies (cdc.gov/art) and based on our parameter and fragmentation analysis, suggest that the transfer of multiple embryos may not be necessary to achieve IVF success.